Algal Research 80 (2024) 103506

Contents lists available at ScienceDirect

Algal Research

journal homepage: www.elsevier.com/locate/algal

Review article

Managing carbon dioxide mass transfer in photobioreactors for enhancing microalgal biomass productivity

Nima Hajinajaf [a,*], Alireza Fallahi [b], Everett Eustance [c], Aditya Sarnaik [a], Anis Askari [d], Mahsa Najafi [e], Ryan W. Davis [f], Bruce E. Rittmann [c], Arul M. Varman [a,*]

[a] Chemical Engineering Program, School for Engineering of Matter, Transport, and Energy, Arizona State University, Tempe, AZ, USA
[b] Biosystems Engineering Department, 200 Corley Building, Auburn University, Auburn, AL 36849, USA
[c] Biodesign Swette Center for Environmental Biotechnology, Arizona State University, Tempe, AZ, USA
[d] Department of Chemical Engineering, Amirkabir University of Technology (Tehran Polytechnic), Tehran, Iran
[e] Department of Chemical Engineering, Vrije Universiteit Brussel, Pleinlaan 2, 1050 Brussel, Belgium
[f] Bioresource and Environmental Security, Sandia National Laboratories, Livermore, CA, USA

ARTICLE INFO

Keywords:
Carbon capture
CO_2 mass transfer
Membrane carbonation
Raceway ponds
Sparger design

ABSTRACT

Mitigating greenhouse-gas emissions, of which fossil-derived carbon dioxide (CO_2) is the dominant component, is becoming increasingly imperative. One of the tools for lowering the demand for fossil carbon is cultivation of microalgae, which are fast-growing photosynthetic microorganisms that utilize sunlight for energy and CO_2 as their carbon source. In addition, microalgae can provide feedstock to replace fossil sources, particularly for transportation fuels. In open and closed microalgal cultivating systems (also called open ponds and photobioreactors, respectively), CO_2 can be sparged into the culture medium through a gas distributor; CO_2 molecules diffuse through the gas-liquid interface and dissolve into the culture medium, from which they can be taken up for the biosynthesis of microalgal cells. Due to the modest solubility of CO_2 in water, optimal design and operating variables (e.g., inlet gas flow rate, sparger characteristics, CO_2 concentration in the inlet gas, and the height of a PBR or sump) are required to increase the CO_2 mass transfer rate into the medium and, consequently, CO_2 uptake and biomass productivity. The concepts and phenomena discussed in this work apply to photobioreactors and open ponds that are sparged with CO_2. This review systematically evaluates how the key design and operating variables affect bubble behavior and the rate of CO_2 delivery into the medium. The review also addresses advanced strategies that are being employed to increase the rate of CO_2 transfer, but with lower costs than with sparging.

1. Introduction

Mitigation of greenhouse-gas emissions, of which carbon dioxide (CO_2) is the dominant component, is becoming increasingly imperative [1–4]. The amount of CO_2 in the atmosphere reached 425 ppm in February 2024, and impacts of global-climate change already are occurring [5], with more severe consequences predicted if the CO_2 concentration exceeds 450 ppm [6,7]. Strategies to reduce atmospheric CO_2 include chemical, physical, and biological CO_2 fixation, and biological methods have environmental and economic advantages [8–10]. CO_2 fixation by terrestrial plants and photosynthetic microorganisms convert CO_2 into organic biomass components [11,12]. Among photoautotrophs, only 3–6 % of global CO_2 is captured by terrestrial plants [12], while CO_2 fixation by microalgae and cyanobacteria is much higher [13,14]. Because microalgae are fast-growing photosynthetic microorganisms that can thrive with simple inputs – sunlight, CO_2, and macronutrients – they are ideal microbial factories for CO_2 uptake and conversion to organic materials of widespread use in society [15–17]. For example, direct air capture (DAC) of CO_2 by microalgae has gained global attention as a simple and scalable option to capture atmospheric CO_2 and turn it into useful products that replace those now produced from fossil sources, such as transportation fuels [18].

Microalgal cultivation can be used to treat wastewater, and it also generates biomass rich in valuable components such as high-value

* Corresponding authors.
E-mail addresses: Nimahajinajaf@gmail.com (N. Hajinajaf), Azf0077@auburn.edu (A. Fallahi), everett.eustance@asu.edu (E. Eustance), rwdavis@sandia.gov (R.W. Davis), Rittmann@asu.edu (B.E. Rittmann), Arul.M.Varman@asu.edu (A.M. Varman).

https://doi.org/10.1016/j.algal.2024.103506
Received 25 August 2023; Received in revised form 5 March 2024; Accepted 9 April 2024
Available online 10 April 2024

nutraceuticals, health-food components, and cosmetics, along with lower-value commodities, such as feedstock for transportation fuel, bioplastics, animal and fish feed, and fertilizer [19–22]. The economics of CO_2 uptake via microalgal cultivation is highly sensitive to biomass productivity per unit area [23]. Identifying conditions that increase productivity will at least partly overcome the economic obstacles [19,24].

Microalgal cultivation systems are divided into open and closed systems. Open systems, such as open raceway ponds, have the advantage of low capital cost and simple construction and operation [25,26]. On the other hand, closed systems can provide better control on cultivation conditions (temperature, pH, light intensity), more efficient CO_2 delivery, minimized water loss, and relatively low invasion by grazers or competitors compared to open systems [27–29]. Disadvantages of closed systems are higher capital and operating costs [30,31], scalability limitations [28,32], and O_2 accumulation [33].

This review focuses on design factors and operating variables that influence the CO_2 availability for microalgal cultivation. The concepts discussed here apply to open and closed systems, for which optimizing the CO_2 delivery can improve biomass productivity, which reduces the overall production costs. We focus on systems in which the CO_2 is delivered by sparging, or the releasing bubbles near the bottom of the water column. This is common for vertical PBR columns and for sumps in an open pond. CO_2 molecules diffuse from the sparged bubbles to become dissolved inorganic-C species that the microalgal cells can fix by photosynthesis. Bubble behavior significantly affects CO_2 transfer into the microalgal suspension, which then influences the microalgal growth and CO_2-capture efficiency. Bubble behavior is affected by many design and operational parameters: e.g., inlet air flow rate, sparger characteristics, CO_2 concentration at the inlet, and the depth of a PBR or sump. This review addresses the effects of the design and operational parameters on bubble behavior and, consequently, the rates of CO_2 uptake and production of valuable products.

2. Fundamentals of microalgal cultivation

Since >50 % of microalgae biomass is comprised of carbon, inorganic C is the most essential input for microalgal growth; inorganic carbon is converted directly into sugars via photosynthesis, and the sugars are then converted into a wide range of organic molecules that constitute biomass [34]. A simple representation of photosynthesis to produce glucose from CO_2 is:

$$6CO_2 + 6H_2O + light\ energy \rightarrow C_6H_{12}O_6 + 6O_2 \quad (1)$$

Glucose is then converted to other biomass components, such as lipids, proteins, nucleotides, pigments, and various other components of biomass. However, the composition of a microalgal cell varies from species to species, as well as with the culture conditions. The average chemical formula for a microalgal cell as reported by Barbosa et al. is $CH_{1.62}O_{0.41}N_{0.14}P_{0.011}$ [35]. The overall equation for the conversion of CO_2 to biomass was obtained by doing an elemental balance and is given by:

$$CO_2 + 0.22\ PO_4^{3-} + 0.14\ NO_3^- + 0.81\ H_2O \rightarrow CH_{1.62}O_{0.41}N_{0.14}P_{0.011} + 1.85\ O_2 \quad (2)$$

Producing 1 ton of algae requires between 1.8 and 2.2 tons of CO_2 [36,37]; an insufficient supply of CO_2 decreases biomass productivity [38]. However, providing excess CO_2 that is unutilized is an economic burden.

2.1. CO_2 chemistry in water

As CO_2 transfers from the gas phase to the liquid phase, it reacts with water and is converted into dissolved inorganic carbon (DIC): (CO_2(aq)), carbonic acid (H_2CO_3), bicarbonate (HCO_3^-), and carbonate (CO_3^{2-}). The speciation is dictated by the pH and alkalinity according to the following chemical equilibria [39]:

$$H_2O + CO_2(aq) \Longleftrightarrow H_2CO_3^* \Leftrightarrow^{K_1} H^+ + HCO_3^- \Leftrightarrow^{K_2} H^+ + CO_3^{2-} \quad (3)$$

in which K_1 and K_2 are the first and second acid-dissociation coefficients. Because, H_2CO_3 dominates $CO_2(aq)$, they are summed and denoted as H_2CO_3* [33] [34]. At near-neutral pH, bicarbonate (HCO_3^-) is the dominant form, and high pH makes carbonate (CO_3^{2-}) the dominant species. Fig. 1 illustrates the pH-controlled speciation.

The concentration of CO_2 present in the aqueous phase at equilibrium is given by Henry's law:

$$C_{CO_2} = \frac{P_{CO_2}}{H_{CO_2}} \quad (4)$$

where C_{CO_2} is the dissolved concentration of CO_2 (mole L^{-1}), P_{CO_2} is the partial pressure of CO_2 in the gas phase (atm), and H_{CO_2} is the Henry's constant for CO_2 (atm L $mole^{-1}$) [40,41]. From Henry's law (Eq. (4)), it is obvious that the gas-phase concentration of CO_2 at the inlet controls the maximum concentration of CO_2 that can be achieved in the liquid phase in the PBR. Therefore, the inlet CO_2 concentration exerts a major control over the CO_2-concentration gradient between the gas phase and the culture medium. In algal-cultivation media, a base level of DIC is typically added in the form of carbonate salts that define the alkalinity. Depending on the cultivation scenario, the alkalinity can range from 1 to 100 mM. Setting the alkalinity and the concentration of CO_2 delivered dictates the equilibrium pH of the cultivation. Fig. 2 highlights the equilibrium DIC concentration based upon these factors. The point at which an alkalinity (alk) line intersects the DIC line based on the CO_2 concentration is the approximate equilibrium point for the cultivation medium.

The Monod model can be used to describe the growth kinetics of microalgae as a function of the concentration of bioavailable inorganic C species, which are H_2CO_3* and HCO_3^- [42].

$$\mu = \mu_{max}\frac{C_y}{K_C + C_y} \quad (5)$$

where C_y is the mM concentration of $H_2CO_3^*$, HCO_3^-, or the sum of $H_2CO_3^*$ and HCO_3^-; μ is the specific growth rate (day^{-1}); μ_{max} is the maximum specific growth rate (day^{-1}); and K_C (in mM) is the Michaelis constant.

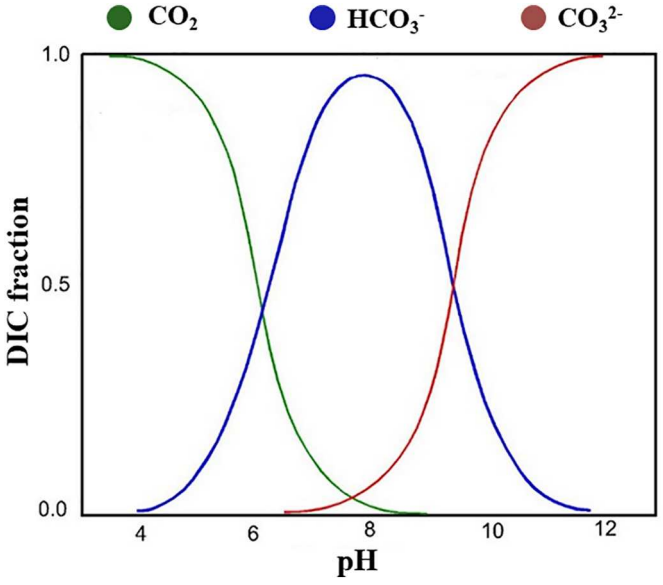

Fig. 1. Dissolved inorganic carbon (DIC) equilibria in the aqueous phase as a function of pH for a temperature of 25 °C.

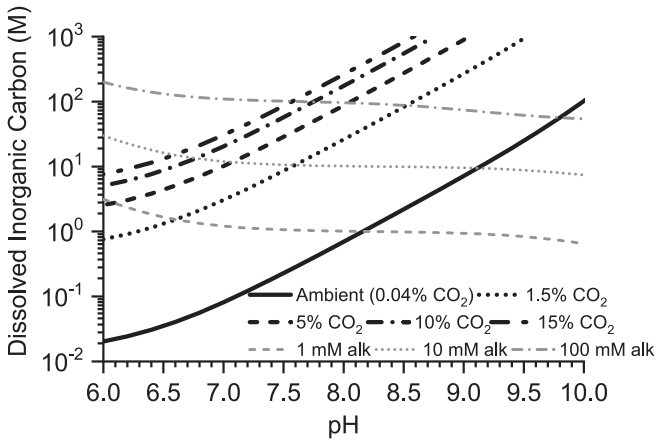

Fig. 2. Available DIC at different pH values based upon the selected alkalinity (alk) and CO_2 concentrations. The intersection of the two factors identifies the equilibrium pH (Modified from Eustance et al. [126]).

The rate of CO_2-mass transfer can be gauged by the increase in DIC.

$$\mathrm{DIC} = \left[H_2CO_3^*\right] + \left[HCO_3^-\right] + \left[CO_3^{2-}\right] \tag{6}$$

The product of the DIC and ionization fractions provides the concentration of each species in the culture medium:

$$\left[H_2CO_3^*\right] = \alpha_1 \cdot DIC \tag{7}$$

$$\left[HCO_3^-\right] = \alpha_2 \cdot DIC \tag{8}$$

$$\left[CO_3^{2-}\right] = \alpha_3 \cdot DIC \tag{9}$$

where the ionization fractions α_1, α_2, and α_3 are calculated from Eqs. (10) to (12) using the pH of the culture medium, where $\mathrm{pH} = -\log[H^+]$.

$$\alpha_1 = \frac{1}{\left(1 + \frac{K_i}{H^+} + \frac{K_i K_j}{(H^+)^2}\right)} \tag{10}$$

$$\alpha_2 = \frac{1}{\left(1 + \frac{H^+}{K_i} + \frac{K_j}{H^+}\right)} \tag{11}$$

$$\alpha_3 = \frac{1}{\left(1 + \frac{(H^+)^2}{K_i K_j} + \frac{H^+}{K_j}\right)} \tag{12}$$

A high pH (>9) favors mass transfer of CO_2 to the liquid medium, because α_1 and the concentration of $CO_2(aq)$ are small; however, most microalgae grow well at pH values of 7 to 9 [43]. Thus, using alkaliphilic microalgal species that can grow well at elevated pH (pH > 10) naturally provides conditions for high CO_2 transfer [44,45], and as an added advantage the high pH environment also provides protection against many grazers and predators that are incompatible with alkaline environments [46].

2.2. Factors affecting CO_2 mass transfer

CO_2 sparged into the medium first diffuses across the gas-liquid interface and rapidly speciates into the various inorganic forms of carbon: CO_2 (aq), carbonic acid (H_2CO_3), bicarbonate (HCO_3^-), and carbonate (CO_3^{2-}), according to the pH. The bioavailable forms of carbon CO_2 (aq) and HCO_3^- can transfer across the cell membrane either through passive diffusion or active transport and then be assimilated by microalgal cells. Carbonic anhydrase (CA) catalyzes the interconversion of CO_2 and HCO_3^- and plays a key role in enhancing carbon transfer through the following steps [47]. First, extracellular CA (eCA) associated with the microalgal cell surface aids in inorganic-carbon uptake by converting HCO_3^- to CO_2 (aq) that readily diffuses across the cell membrane into cytoplasm and then to chloroplast [48,49]. Although, passive diffusion of CO_2 into the cell due to its high solubility in lipid membranes has the benefit of energy saving for the cell, CO_2 can also diffuse out of the cell. To overcome this, in its second role, CA present within the cytoplasm and chloroplast converts CO_2 to HCO_3^-, which then enters the pyrenoid, a major compartment in chloroplast. The effectiveness of microalgal photosynthesis is credited to the CO_2-concentrating mechanism (CCM), which is facilitated by the CA present in the pyrenoid. In the final step, CA present within the pyrenoid converts HCO_3^- to CO_2, thereby concentrating the localized concentration of CO_2 in the proximity of RuBisCO to enhance the rate of CO_2 fixation [50,51]. This process is shown schematically in Fig. 3.

The CO_2-transfer rate (N_{CO_2}, mol m^{-3} min^{-1}) from the gas phase to the liquid phase at any location is given by

$$N_{CO_2} = k_l a \times \nabla \mathrm{CO_2} \tag{13}$$

where k_La is the overall volumetric mass-transfer coefficient (min^{-1}), k_L is the mass-transfer coefficient (m min^{-1}); a is the interfacial area per unit volume (m^{-1}), and ∇CO_2 is the CO_2-concentration gradient between the gas and the aqueous phase (mol m^{-3}). Eq. (14) can be used to obtain the total amount of CO_2 transferred to the culture medium:

$$\mathrm{Q} = N_{CO_2} \times V_{PBR} \times \Delta t \tag{14}$$

where Q is the total CO_2 transferred to the culture media (mol), V_{PBR} is the working volume of the photobioreactor (m^3), and Δt is time (min).

The value of k_La is affected by bubble behavior, the superficial gas velocity, sparger design, temperature, and culture-medium properties. Therefore, the design and operational parameters of the PBR or sump, including the inlet CO_2 concentration, sparger design, and inlet gas flow rate, affect k_La and, as a consequence, the CO_2-mass transfer rate, as illustrated in Fig. 4. The influence of these factors is discussed in Section 3.

3. Photobioreactor design variables

3.1. Inlet CO_2 concentration

The inlet CO_2 concentration is an important variable in the design of PBRs, as it affects the driving force available for CO_2 transport from the gas phase to the liquid phase. Depending on reactor design and available gas sources, the concentration of CO_2 can vary from <1 % (e.g., from air) to 100 % CO_2 (e.g., from pure CO_2 or from fermentation off-gas). In some scenarios, the concentration of CO_2 being utilized can be manipulated to a desired concentration. However, algal cultivation can be integrated with an industrial process that produce waste CO_2. For example, natural-gas and coal-fired power plants produce waste streams containing 3–8 % and 10–15 % CO_2, respectively [52]. In contrast, biogas from anaerobic digesters and landfills have 30–40 % CO_2 typically.

The CO_2 concentration in the CO_2-delivery gas dictates the concentration gradient and, therefore, the rate at which CO_2 can be transferred to the culture medium. As the bubbles rise, they decrease in size based upon the change in their CO_2 concentration and initial bubble size [53,54]. This, in turn, affects the bubble-rise velocity and residence time, as smaller bubbles have a slower velocity [55,56]. In addition, bubble-rise trajectory, bubble-growth rate, and bubble-detachment rate are influenced by the inlet CO_2 concentration [54,56]. For example, Zhao et al. [57] observed that, as the CO_2 concentration was increased from 10 % to 20 %, the rate of bubble growth decreased due to a higher CO_2 gradient between the gas and the aqueous phase, leading to enhancement in CO_2 mass transfer. Ding et al. [56] also showed that injecting gas with a higher CO_2 concentration caused the bubbles to have less acceleration on their rise velocity, which led to a lower

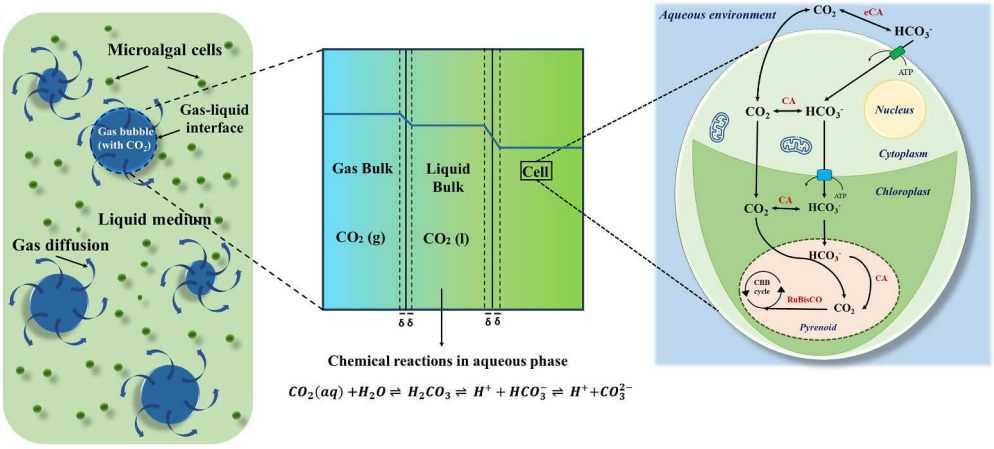

Fig. 3. CO_2 mass transfer from a bubble to a microalgal cell and the mass-transfer resistances encountered in each step. The bioavailable forms (CO_2 and HCO_3^-) can transfer across the cell membrane and be assimilated by microalgal cells either through passive diffusion or active transport. Carbonic anhydrase (CA) functions vitally in transforming two primary forms of CO_2 and HCO_3^- together. This process enhances the targeted active transport of HCO_3^- to the pyrenoid in microalgae.

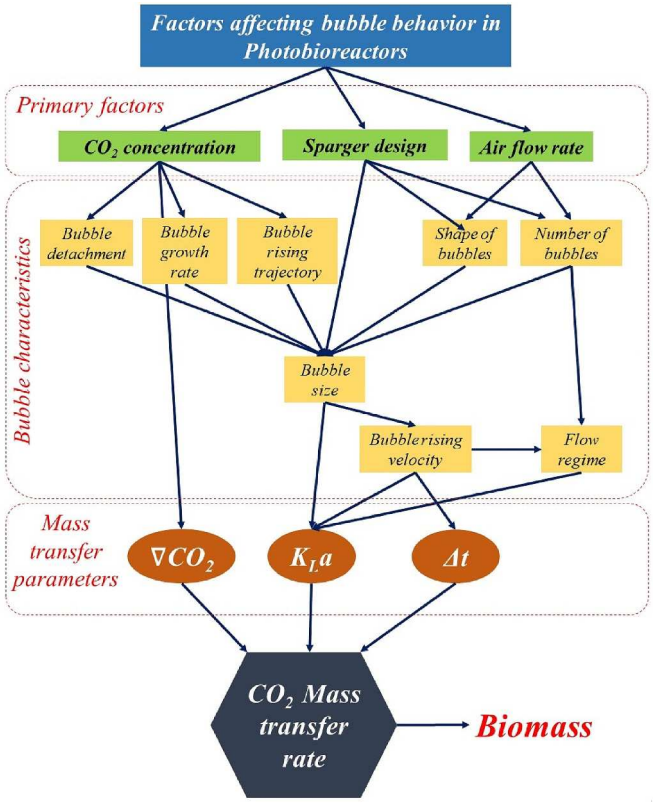

Fig. 4. Schematic of how CO_2 concentration, sparger design, and gas-flow rate affect bubble behavior, mass transfer parameters, and, thereby, CO_2-mass transfer to the microalgae-culture medium in a PBR.

terminal velocity. These observations emphasize the fact that the inlet CO_2 concentration is an important variable to control CO_2 mass transfer in a PBR.

Inlet CO_2 concentration and its effect on microalgal growth. Although a higher input CO_2 concentration favors CO_2 mass transfer, providing higher CO_2 concentrations also can lower the pH of the culture, as the medium's alkalinity is distributed to a larger pool of DIC [42]. Thus, a proper balance between CO_2 concentration and pH has to be established to optimize microalgal growth. For example, Barahoei et al. [58] showed that increasing the input CO_2 concentration from 3 % to 7 % boosted biomass productivity by 57 %, which is consistent with other published studies [59–61]. In another work, *Chlorella* sp. was cultivated with CO_2 concentrations ranging from 10 to 25 % [62], and 10 % CO_2 was observed to yield maximal growth. On the other hand, Ding et al. [63] found that the maximum growth rate for *Chlorella pyrenoidosa* occurred when the CO_2 concentration was 5 %. They explained that concentrations below 5 % led to limitation from CO_2 mass transfer, but concentrations above 5 % lowered the pH enough to have a negative influence on the microalgal growth rate.

pH-stat. In cultivation conditions in which CO_2 is delivered separately from coarse aeration or is blended into a single gas stream, excessive CO_2 levels, which acidify the culture medium, can be mitigated through pH control [64]. Fig. 2 supports that, depending on CO_2 availability in the gas phase and culture-medium alkalinity, a targeted pH set point can maximize CO_2 mass transfer without acidifying the medium.

Bubble behavior as a function of CO_2 concentration and column height. The height of the photobioreactor also affects bubble-residence time, which affects mass transfer of CO_2 to the culture. A desirable height of a photobioreactor requires a proper height/diameter ratio, which depend on economics and the impact of CO_2 concentration and column height on bubble behavior. Therefore, we look at bubble behavior for two scenarios: (i) a fixed column height, but varying inlet CO_2 concentration (Fig. 5a); and (ii) a fixed inlet CO_2 concentration, but varying column height (Fig. 5b).

For bubbles rising in a quiescent liquid, three forces simultaneously control the bubble's behavior: buoyancy, drag, and gravitational force. Near the gas entry point at the bottom of the water column, buoyancy dominates, resulting in bubble acceleration. However, as the bubble accelerates up through the water column, the drag force increases. As the bubble reaches a certain height, the net force acting on the bubble equals zero, at which point the bubble attains its terminal velocity [63].

For a fixed height (Fig. 5a), increasing the inlet CO_2 concentration decreases the bubble diameter as the bubble rises and loses CO_2, consequently decreasing the bubble-rise velocity [63]. Smaller bubbles and increased partial pressure of CO_2 increase the CO_2 transport rate [65], as well as the rate at which the bubble size shrinks as it rises; this is illustrated in Fig. 5a.

As the bubble travels upward, the partial pressure of CO_2 in the bubble decreases, and, as a consequence, the partial pressures of other gases (e.g., N_2 and O_2) increase. The bulk of air is N_2, but microalgal photosynthesis produces O_2, which accentuates the increase of O_2 partial pressure in the bubble as it travels up through the reactor. Transfer of O_2 into the bubbles can be a benefit, since it is well established that high dissolved O_2 concentration inhibits microalgal growth [66,67]. For

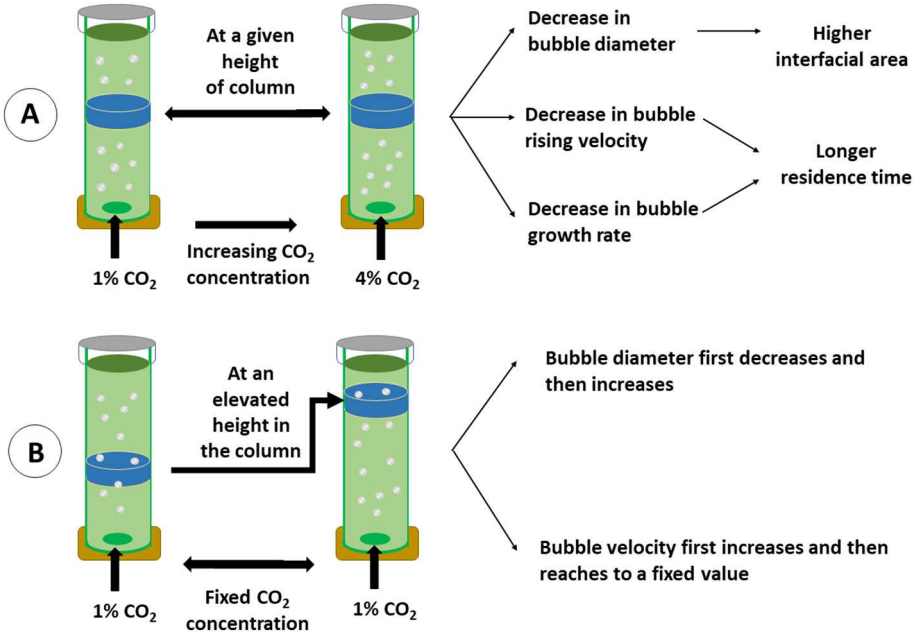

Fig. 5. Factors affecting bubble behavior for two conditions: a) at a given height of photobioreactor with different CO_2 concentrations, and b) at a fixed CO_2 concentration for different column heights.

example, dissolved-oxygen concentrations over 30 mg L^{-1} led to a 30 % loss in biomass productivity in *Chlorella vulgaris*. Therefore, mitigation of dissolved-O_2 buildup may be required for optimal design, especially in large-scale tubular photobioreactors [68,69]. One strategy is to supply CO_2 at a higher concentration, which simultaneously increases CO_2 mass transfer to the medium and O_2 transfer from the medium to the bubbles.

Optimal CO_2 concentration depends on cultivation conditions. Although some earlier studies showed that inlet-CO_2 concentrations above 5 % harmed microalgal cells and inhibited their growth [70–72], more recent studies underscored the benefits of higher inlet CO_2. Tongprawhan et al. [73] sparged gas with air (0.03 % CO_2) and 50 % CO_2 and observed 3 times faster growth with 50 % CO_2. Similarly, Tang et al. [61] cultivated *Scenedesmus obliquus* (SJTU-3) and *Chlorella pyrenoidosa* (SJTU-2) with CO_2 ranging from 0.03 % to 50 % and observed optimal growth at 10 % CO_2 concentration. Others saw the fastest growth of microalgae using 50 % and 100 % CO_2 in concert with a pH stat to control the pH [74–76]. An overview of the results obtained by notable studies is provided in Table 1. Taken together, these results indicate that maximizing CO_2 utilization in microalgal cultivation requires careful co-optimization of the inlet CO_2 concentration, microalgal species, pH/alkalinity, equipment, and operating conditions that affect bubble size dynamics, including the diameter-to-height ratio and the superficial gas velocity.

3.2. Gas flow rate and superficial gas velocity

The gas flow rate (Q_g, m^3 min^{-1}) is an independent parameter that affects the amount of CO_2 that can be transferred to the culture medium. The gas flow rate directly determines the superficial gas velocity, $U_g = Q_g/A_{cs}$, where A_{CS} is the cross-sectional area of the column (m^2). The bubble residence time is strongly affected by U_g, because U_g has a direct impact on bubble diameter and shape [77–79], as well as the number of bubbles formed [80]. Low superficial gas velocities ($U_g < 0.03$ m s^{-1}) allow bubbles to aggregate to form larger bubbles that have a higher rising velocity [63,78,79,81]. In contrast, large superficial gas velocities ($U_g > 0.05$ m s^{-1}) leads to the breakup of large bubbles into smaller bubbles that rise more slowly.

Besides the impact of U_g on bubble size and CO_2 mass transfer, selection of a proper superficial gas velocity is especially crucial at higher cell densities in PBRs, because it also controls mixing and the spatial distribution of the cells. At high cell densities, cells at the center of the PBR column will be shaded by cells at the periphery. A high-enough U_g allows all cells to be exposed to light, and it also prevents cells from settling at the bottom of the column or sticking to the column wall. Proper mixing also ensures homogeneous distribution of nutrients in the PBR and maintains a uniform temperature and pH [10,82]. On the other hand, too-high superficial gas velocity has two negative impacts. First, it can cause excessive shear stress on the microalgal cells, which has been observed with *Spirulina platensis* [83], *Dunaliella* [84], *Tetraselmis suecica* [85], *Gymnodinium splendens* [86], and others [83]. Second, bubbles scatter light, and more bubbles increase light attenuation [57].

3.3. Spargers

Sparging has two functions: mixing of algal cells (especially in PBRs) to utilize light efficiently and gas transfer for CO_2 delivery and O_2 removal. Sparging is affected by the sparger type (summarized in Table 2) and the gas-flow rate (Q_g, m^3 min^{-1}), which collectively dictate bubble size, the number of bubbles, and overall mixing intensity. A large trade-off of sparging is related to bubble size::arge bubbles are better for mixing, while smaller bubbles offer better gas transfer. Bubble size is dictated by the sparger orifice diameter and total gas flow rate. Coarse aeration is typically produced by orifices ≥1 mm and generates bubbles that are ≥5 mm [87], while fine aeration generates bubbles that can be classified into macrobubbles (>100 μm), microbubbles (1–100 μm), and nanobubbles (<1 μm) [88]. Fig. 6 depicts the impact of sparger pore size and flow rate on bubble size in a PBR.

Smaller bubbles have an increased surface-area-to-volume ratio and a slower rise velocity compared to larger bubbles, which increases the overall interfacial area (a) in the mass transfer coefficient (k_La) and allows for more efficient CO_2 delivery [89]. For example, microbubbles have been shown to improve mass transfer per flow rate by up to 100-fold, compared to aquatic, industrial, and open-tube spargers [90]. Nanobubbles have even greater surface area and do not rise at all due to the virtual disappearance of buoyant force [91]. However, generating microbubbles and nanobubbles increases energy costs by a factor of four over coarse aeration, although this cost may be offset by the increase in CO_2 transfer efficiency [4,92]. In addition, using microbubbles or

Table 1
A review of previous studies regarding the effects of design and operating parameters on biological CO_2 uptake.

Species	Cultivation system and volume (L)	Sparger type	Flow rate (mL/min, vvm[a])	Inlet CO_2 concentration (%) (ppm)[b]	Mass transfer coefficient (h^{-1})	Maximum Biomass Concentration ($g.L^{-1}$)	Biomass productivity ($g.L^{-1}.d^{-1}$)	Optimal conditions reported	CO_2 removal (% w/w) (mg. $L^{-1}.h^{-1}$)[a]	Ref.
Chlorella vulgaris	Bubble column PBR (4)	Spiral	50 mL/min (0.0125 vvm) 50 mL/min (0.0125 vvm) 150 mL/min (0.0375) 150 mL/min (0.0375)	0.04 15 0.04 15		1.75 3.15 1.92 2.29	0.31 0.35 0.24 0.23	100 mL/min 7.52 % CO_2		[8]
Chlorella vulgaris	Bubble column PBR (9.6)	Spiral	100 mL/min (0.0104 vvm)	7.52		3.43	0.41	100 mL/min 7.52 % CO_2		[8]
Chlorella vulgaris	Bubble column PBR (16)	Spiral	50 mL/min (0.0031 vvm) 50 mL/min (0.0031 vvm) 150 mL/min (0.0094 vvm) 150 mL/min (0.0094 vvm)	0.04 15 0.04 15		1.79 3.13 2.2 3.25	0.25 0.38 0.33 0.49	100 mL/min 7.52 % CO_2		[8]
Chlorella PY-ZU1	Plate PBR (21)	Jet aerator	0.02 vvm 0.04 vvm 0.06 vvm 0.08 vvm 0.1 vvm	15	32 39 48 49 50	1.33	–	–	–	[108]
Synechococcus elongatus	Membrane sparger PBR (0.013)	Polypropylene hollow fiber membrane sparger	25 mL/min (1.9 vvm)	0.04 5 10	1.49 1.86 2.28	1.86 2.45 1.51	0.86 1.23 0.48	5 % CO_2	32 4	[109]
Synechococcus elongatus	Membrane contactor PBR (0.04)	Polypropylene hollow fiber membrane contactor	25 mL/min (0.625 vvm)	0.04 5 10	1.25	1.78 1.92 2.1	0.75 0.96 1.12	10 % CO_2	10 25	[109]
Chlorella sp. *AG10002*	Bubble column PBR (0.6)	Gas sparger	0.06 vvm 0.1 vvm 0.2 vvm 0.4 vvm	0.5 1 2 5	–	1.16 1.54 1.78 2.02	0.191 0.255 0.295 0.335	0.2 vvm 5 % CO_2	83.3 [a] 112.5 129.1 145.8	[60]
Chlorella vulgaris	Bubble column PBR (1)	Gas sparger	1 vvm	0.03 1 5 10 15	–	2.71 3.32 3.76 2.59 0.65	0.72 0.9 1.01 0.69 0.15	0.5 vvm 5 % CO_2	–	[110]
Chlorella vulgaris	Bubble column PBR (1)	Gas sparger	0.1 vvm 0.5 vvm 1 vvm 1.5 vvm 2 vvm	5	–	2.95 3.83 3.51 2.54 1.07	0.84 1.07 0.95 0.67 0.32	0.5 vvm 5 % CO_2	–	[110]
Chlorella vulgaris	Bubble column PBR (5)	PVDF hollow fiber membranes with internal diameter of 0.5 mm	1.2 L/min (0.24 vvm)	0.5 1 6 12	–	0.65 0.75 0.60 0.59	–	1 % CO_2	37[a] 62 180 80	[111]
Chlorella vulgaris	Bubble column PBR (0.5)	Gas sparger		0.03 3 5 7	–	0.47 0.88 0.82 1.11	0.07 0.13 0.12 0.16	5.35 % CO_2	43.36 41.78 41.64 42.44	[112]

(*continued on next page*)

Table 1 (*continued*)

Species	Cultivation system and volume (L)	Sparger type	Flow rate (mL/min, vvm*)	Inlet CO_2 concentration (%) (ppm)[b]	Mass transfer coefficient (h^{-1})	Maximum Biomass Concentration ($g.L^{-1}$)	Biomass productivity ($g.L^{-1}.d^{-1}$)	Optimal conditions reported	CO_2 removal (% w/w) ($mg.L^{-1}.h^{-1}$)[a]	Ref.
				9		1.03	0.15		42.83	
				10		1.01	0.15		49.09	
Pseudokirchneriella subcapitata	Bubble column PBR (0.5)	Gas sparger		0.03	–	0.48	0.08	4.87 % CO_2	46.22	[112]
				3		0.79	0.12		45.91	
				5		0.65	0.10		45.67	
				7		0.66	0.10		42.84	
				9		0.90	0.13		41.94	
				10		0.53	0.18		37.19	
Synechocystis salina	Bubble column PBR (0.5)	Gas sparger		0.03	–	0.46	0.07	5.55 % CO_2	43.04	[112]
				3		0.10	0.15		42.32	
				5		0.92	0.14		42.21	
				7		1.15	0.17		41.56	
				9		0.97	0.14		43.00	
				10		0.75	0.11		42.19	
Microcystis aeruginosa	Bubble column PBR (0.5)	Gas sparger		0.03	–	0.38	0.06	5.62 % CO_2	42.75	[112]
				3		0.87	0.13		42.20	
				5		0.88	0.14		42.68	
				7		1.01	0.15		42.29	
				9		0.84	0.12		40.50	
				10		0.81	0.12		42.05	
Chlorella vulgaris	Bubble column PBR (5)	–	–	0.03	–	0.50	–	5 % CO_2	92.2	[113]
				0.5		0.54			7.1	
				1		0.69			4.5	
				2		0.69			2.5	
				5		1.16			1.5	
Spirulina platensis	Flat plate (10)	–	–	0.03	–	0.52	–	10 % CO_2	13.75 [a]	[114]
				2		0.64			16.66	
				5		0.70			18.33	
				10		0.72			18.75	
Chlorella vulgaris	Flat plate (10)	–	–	0.03	–	0.46	–	10 % CO_2	3.75 [a]	[114]
				2		0.60			5	
				5		0.64			5.41	
				10		0.70			5.83	
Chlorella pyrenoidosa	Bubble column (0.4)	–	20 mL/min (0.05 vvm)	3	–	1.30	–	%5 CO_2 20 mL/min	–	[63]
			10 mL/min (0.025 vvm)	5		1.26				
			20 mL/min (0.05 vvm)	5		1.53				
			30 mL/min (0.075 vvm)	5		1.48				
			20 mL/min (0.05 vvm)	10		1.21				
Chlorella sp. FC2 IITG	Bubble column (10)	Porous flexi-membrane rubber strip aerator	0.08 vvm	2	–	4.26	0.27	–	–	[115]
Chlorella mutant PY-ZU1	Horizontal tubular PBR (0.11)		0.1 vvm	15	6.0	3.84	–	–	–	[116]
			0.2 vvm		8.5					
			0.3 vvm		10.1					
			0.4 vvm		11.5					
			0.5 vvm		12.1					
Chlorella mutant PY-ZU1	Horizontal tubular PBR (0.11)	Ceramic shell aerator	0.1 vvm	15	10.1	5.4	–	–	–	[116]
			0.2 vvm		13.5					
			0.3 vvm		15.0					

(*continued on next page*)

Table 1 (*continued*)

Species	Cultivation system and volume (L)	Sparger type	Flow rate (mL/min, vvm*)	Inlet CO_2 concentration (%) (ppm)[b]	Mass transfer coefficient (h^{-1})	Maximum Biomass Concentration ($g.L^{-1}$)	Biomass productivity ($g.L^{-1}.d^{-1}$)	Optimal conditions reported	CO_2 removal (% w/w) ($mg.L^{-1}.h^{-1}$)[a]	Ref.
			0.4 vvm		16.5					
			0.5 vvm		19.0					
Scenedesmus Sp.	Multicultivator (0.14)	Diffuser with diameter of:			–			6.02 % CO_2	–	[117]
		0.4 mm	1.5 vvm	50000[b]		4.69	0.29	0.39 vvm 4.0 mm diameter diffuser		
		1 mm	0.5 vvm	20000[b]		3.95	0.29			
		2.6 mm	1.5 vvm	50000[b]		4.45	0.38			
		4 mm	3vvm	20000[b]		2.69	0.27			
		5 mm	1.5 vvm	50000[b]		4.77	0.29			
Scenedesmus dimorphus	Flat-plate PBR (4.27)	Air di users made of sintered glass (average pore diameter 0.16)	0.05vvm	14.10	0.5	3.8	0.29	–	14	[118]
			0.10vvm		0.7	4.7	0.44		64	
			0.15vvm		1.2	3.4	0.22		11	
Euglena gracilis (CCAP1224/5Z)	Erlenmeyer flasks (0.5)	–	0.3 L/min (0.6 vvm)	2.30	–	1.4	–	–	10	[119]
Phaeodactylum tricornutum (CCAP1055/1)	Erlenmeyer flasks (0.5)	–	0.3 L/min (0.6 vvm)	0.04	–	0.87	–	–	65	[119]

[a] CO_2 removal ($mg.L^{-1}.h^{-1}$).

[b] Inlet CO_2 concentration (ppm).

* vvm - volume of air sparged (in aerobic cultures) per unit volume of growth medium per minute.

nanobubbles can improve light-utilization efficiency in low-density cultures, because smaller bubbles disperse light more effectively and homogeneously [57].

Dual sparging. Because of the value of having large and small bubbles in sparged algal cultures, Eriksen et al. [93] proposed using dual sparging in bubble column. This approach allows for coarse-bubble aeration with air to provide the needed mixing for light utilization, while using fine bubbles for enhanced CO_2 mass transfer. This approach increased the fraction of CO_2 transferred into the liquid phase from 11 % to 55 %, while also maintaining the same growth rate. Because the small bubbles were 100 % CO_2, they provided the maximum driving force for transferring the CO_2 into the culture medium.

Energy demand for sparging. The measurement of specific power consumption (P/V) entails evaluating the energy consumption for each unit volume of liquid in the photobioreactor (V). This calculation of P/V takes into account the overall decrease in gas pressure (ΔP) as well as the rate at which gas is flowing into the reactor (Qp) that is described in Eq. (15) [94–96]:

$$\frac{P}{V} = Q_P \frac{\Delta P}{V} \tag{15}$$

The energy to sparge algal cultures depends on two factors: 1) the depth of the sparger and 2) the frictional loss associated with the sparger design. The head loss from the sparger is the sum of the head loss in the pipe leading to the sparger and the head loss through the orifices. The total head loss across the pipe and a single orifice can be calculated by using Eq. (16) [94]:

$$\Delta h = f_d \cdot \frac{L}{2g} \cdot \frac{V^2}{D} + \frac{V_\circ{}^2 - V^2}{\left(2gC_\circ{}^2\right)} \tag{16}$$

where Δh is the head loss (m), f_D is the Darcy-Weisbach friction factor (dimensionless), L is the pipe length (m), D is the hydraulic diameter of the pipe (m), g is the gravitational constant ($m\ s^{-2}$), V is the mean flow velocity through the pipe ($m\ s^{-1}$), $V_\circ$ is mean flow velocity through the orifice ($m\ s^{-1}$), and $C_\circ$ is orifice coefficient which is correlated to the ratio of sparger diameter to pipe diameter. Eq. (15) is a simplified equation for a single orifice, however, for practical scenarios, the mathematical form for head loss across sparger varies by the type of sparger used, number of orifices, distance of orifice from each other, nozzle shape, etc. It can be noted from Eq. (15) that head loss increases with a decreasing orifice size and increasing gas flow velocity. Furthermore, for a fixed gas volumetric flow rate, decreasing the orifice diameter also leads to an increase in the gas flow velocity, unless the number of orifices is increased to account for the smaller area per orifice. Table 2 summarizes the various types of spargers used and the associated trade-offs that occur with their implementation in microalgal cultivation.

The pressure drop is further affected by the sparger-design variables: 1) sparger type (e.g., sintered glass, porous sparger, perforated plate, ring, pipe and nozzle sparger) [97]; 2) number of orifices and their diameter [79]; 3) pitch, the distance between orifice [98,99]; and 4) sparger positioning in the water column (more pressure deeper in the water column) [100].

Other sparger-design factors. Minimizing bubble weeping and non-uniformity are two other crucial aspects for designing an effective sparger [101]. Weeping arises when the sparger pressure is low in comparison to the static pressure exerted by the culture medium; then, water can enter the sparger orifices, leading to clogging, fouling, and, consequently, increased pressure drop. Non-uniformity occurs when the air flow rate along the length of the sparger is not uniform, and it also can lead to water intrusion in the low-pressure areas. These problems can be overcome by maintaining a sufficient pressure across the sparger.

Table 2
The most common types of spargers used in PBRs and their positive and negative characteristics.

Sparger type	Positive characteristics	Negative characteristics	References
Plate	• Widely used • Simple design	• Produces coarse bubbles • Maldistribution across the pores • Thick plate spargers usually have high pressure drop	[120]
Pipe	• Commonly used in microalgal cultivation • Produces small bubbles with proper spacing and hole diameter	• Uneven gas output and mixing in the reactor	[60,121]
Multiple-ring and spider	• Good with high superficial gas velocity	• Non-uniform bubbles	[122]
Wheel type	• Relatively uniform bubbles • Eliminates the need for several pipes in a sparger	• Only suitable for the limited range of operating parameters	[123]
Ceramic airstone	• Creates fine bubbles	• Smaller bubble size may result in some cell damage	[124]
Porous membranes	• Large gas-liquid contact area • Small bubbles	• Pores easily blocked • Relatively short lifespan	[75,125]

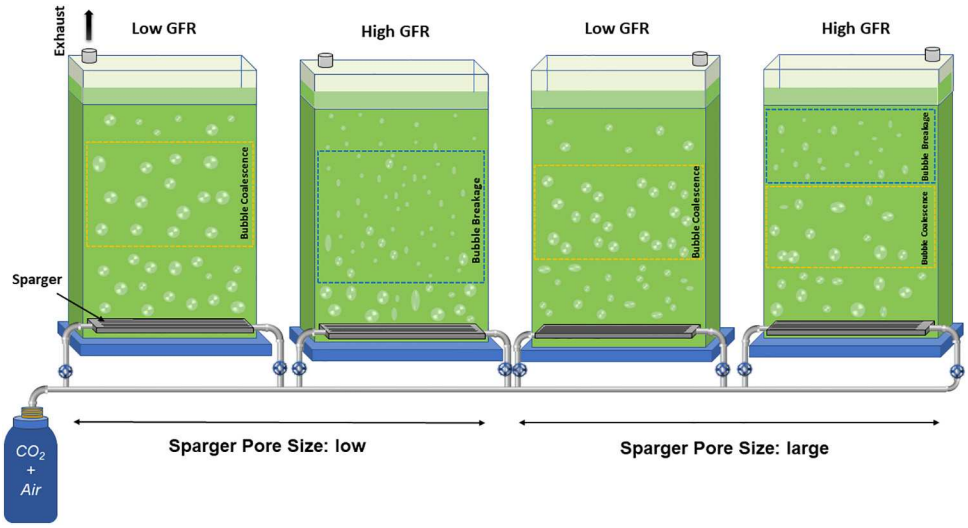

Fig. 6. Effect of sparger pore size and gas flow rate (GFR) on bubble size and behavior in a photobioreactor. Bubble coalescence and bubble breakage regime in the photobioreactor under various conditions have been depicted. Note: The size of bubbles depicted in this image are only for the purpose of illustrating trends.

4. Advanced technologies to increase CO_2 mass transfer

High CO_2 mass-transfer kinetics and utilization efficiency are critical for reducing operating costs. Carbon utilization efficiency (CUE) is the percentage of delivered CO_2-C that is fixed into biomass-C. Another metric is the carbon-transfer efficiency (CTE), which is the percentage of delivered CO_2-C that is retained in biomass and in the medium's IC. The relationship between CUE and CTE primarily depends of pH, as a higher pH leads to a higher IC concentration. Current sparging techniques often give low CUEs, often <20 %, and low CTEs, often <30 % [74,102]. Much higher CUEs and CTEs are needed to make CO_2 delivery cost-effective: for example, a target is 80 % CUE [74], which translates to a CTE of 80–90 %.

Current research into improving the mass transfer of CO_2 into algal cultures can be split into 3 categories: biological/enzymatic (carbonic anhydrase), chemical (pH), and physical (membrane carbonation).

Carbonic anhydrases (CA) are a ubiquitous group of metalloenzymes that catalyze the rapid inter-conversion of CO_2 to HCO_3^- [103]. Microalgal cells utilize internal and external CAs to as a part of their carbon-concentrating mechanism to increase the efficiency of CO_2 fixation. Overall, using CAs can be utilized in PBR to increase carbon capture and biomass productivity. However, CAs have numerous limitations including, poor stability and low recovery of enzymes. Therefore, CAs are being immobilized on buoyant or submerged substrata to enhance stability and for ease of recovery [104–106]. In addition, research over the past decade has focused on finding or developing novel CAs that have increased robustness in real-world conditions [107].

One of the most common approaches to increasing the mass transfer of CO_2 is to utilize highly alkaline environments (pH >10), which allows for the direct reaction of CO_2 with hydroxide ions to produce HCO_3^-. To account for the conversion of CO_2 to HCO_3^-, an enhancement factor (E_1) is introduced to Eq. (17) [46].

$$N_{CO_2} = E_1 \times k_l a \times \nabla CO_2 \quad (17)$$

Depending on pH, E_1 can range from 20 at pH 9.5 to 170 at pH 10.3. However, operating at high pH requires alkaliphilic algal species, such as *Spirulina*. E1, is related to the reaction kinetics that drive the direct conversion of CO_2 and OH- into HCO_3^-, which is significantly faster than the when CO_2 reacts with H_2O to generate H_2CO_3.

Similar to reducing bubble size, another option to increase "*a*" is membrane carbonation (MC), which utilizes non-porous hollow-fiber membranes to mediate the transfer of gaseous CO_2 into the culture medium without the formation of bubbles [74,75]. By utilizing bubble-free CO_2 delivery, MC can achieve nearly 100 % CTE, since bubble loss is precluded. Research has shown that MC with pure CO_2 is capable of rapidly delivering CO_2 to algae raceways with no difference in pH or growth rates compared to conventional sparging, but with a much higher CTE and CUE (e.g., ~100$ and ≥80 %, respectively) [74].

5. Conclusion

Microalgal photosynthesis is a promising approach for utilizing gas-phase CO_2 to provide feedstock for biobased commodities. Because rapid microalgal photosynthesis creates a large demand for IC, maintaining a

sufficient concentration of dissolved IC is essential to support the growth of the microalgae. Therefore, microalgal-cultivation systems must be designed to provide high-rate and high-efficiency CO_2 mass transfer, and transfer of CO_2 from bubbles to the liquid is the most common approach. Fundamentally, the rate of mass transfer of CO_2 depends on the CO_2-concentration gradient between the bubbles and the liquid medium, the bubble surface area, and the bubble residence time. The transer of CO_2 to the liquid medium is increased by a high inlet CO_2 concentration (a high concentration gradient), fine bubbles (high surface area and longer residence time) and a greater water column depth (longer bubble residence time). However, each of these accelerating factors can increase operating costs. Therefore, other strategies are being investigated to minimize the capital and operational costs; e.g., using carbonic anhydrases, high pH with alkaliphilic phototrophic microorganisms, and membrane carbonation.

CRediT authorship contribution statement

Nima Hajinajaf: Conceptualization, Data curation, Supervision, Visualization, Writing – original draft, Writing – review & editing. **Alireza Fallahi:** Conceptualization, Data curation, Visualization, Writing – original draft, Writing – review & editing. **Everett Eustance:** Conceptualization, Writing – original draft, Writing – review & editing. **Aditya Sarnaik:** Conceptualization, Visualization, Writing – original draft, Writing – review & editing. **Anis Askari:** Data curation, Writing – original draft, Writing – review & editing. **Mahsa Najafi:** Writing – original draft, Writing – review & editing. **Ryan W. Davis:** Funding acquisition, Supervision, Writing – review & editing. **Bruce E. Rittmann:** Conceptualization, Writing – original draft, Writing – review & editing. **Arul M. Varman:** Conceptualization, Funding acquisition, Supervision, Writing – original draft, Writing – review & editing.

Declaration of competing interest

The authors declare that they have no known competing financial interests or personal relationships that could have appeared to influence the work reported in this paper.

Data availability

Data will be made available on request.

Acknowledgment

AMV acknowledges start-up funds from the School for Engineering of Matter, Transport and Energy at Arizona State University. This research was also supported in part by Sandia National Laboratories through awards #2184871 and #1871463, and in part by the National Science Foundation through award #CBET-2146114 to AMV. This research was also supported in part by the BioEnergy Technology Office (BETO), U.S. Department of Energy, through support of RWD, under agreement #26336.

References

[1] S.R. Chia, et al., CO2 mitigation and phycoremediation of industrial flue gas and wastewater via microalgae-bacteria consortium: possibilities and challenges, Chem. Eng. J. 425 (2021) 131436.
[2] A. Fayyazbakhsh, et al., Engine emissions with air pollutants and greenhouse gases and their control technologies, J. Clean. Prod. (2022) 134260.
[3] W. Kong, et al., Review on carbon dioxide fixation coupled with nutrients removal from wastewater by microalgae, J. Clean. Prod. 292 (2021) 125975.
[4] M.D. Somers, J.C. Quinn, Sustainability of carbon delivery to an algal biorefinery: a techno-economic and life-cycle assessment, J. CO2 Util. 30 (2019) 193–204.
[5] Earth's CO2, 2022.
[6] A. Fischlin, et al., Ecosystems, Their Properties, Goods and Services, 2007.
[7] A.E.R. Hassoun, et al., The carbonate system of the eastern-most Mediterranean Sea, Levantine sub-basin: variations and drivers, Deep-Sea Res. II Top. Stud. Oceanogr. 164 (2019) 54–73.
[8] N. Hajinajaf, et al., Integrated CO2 capture and nutrient removal by microalgae Chlorella vulgaris and optimization using neural network and support vector regression, Waste Biomass Valoriz. (2022) 1–22.
[9] S.-H. Ho, et al., Perspectives on microalgal CO2-emission mitigation systems — a review, Biotechnol. Adv. 29 (2) (2011) 189–198.
[10] A. Kumar, et al., Enhanced CO2 fixation and biofuel production via microalgae: recent developments and future directions, Trends Biotechnol. 28 (7) (2010) 371–380.
[11] O. Pulz, W. Gross, Valuable products from biotechnology of microalgae, Appl. Microbiol. Biotechnol. 65 (6) (2004) 635–648.
[12] K. Skjånes, P. Lindblad, J. Muller, BioCO2–a multidisciplinary, biological approach using solar energy to capture CO2 while producing H2 and high value products, Biomol. Eng. 24 (4) (2007) 405–413.
[13] A. Hashemi, et al., CO2 biofixation by Synechococcus elongatus from the power plant flue gas under various light–dark cycles, Clean Techn. Environ. Policy 22 (8) (2020) 1735–1743.
[14] J.A.V. Costa, et al., Modelling of growth conditions for cyanobacterium Spirulina platensis in microcosms, World J. Microbiol. Biotechnol. 16 (1) (2000) 15–18.
[15] N. Hajinajaf, et al., Experimental and modeling assessment of large-scale cultivation of microalgae Nannochloropsis sp. PTCC 6016 to reach high efficiency lipid extraction, Int. J. Environ. Sci. Technol. (2022) 1–18.
[16] J. Sheehan, et al., Look Back at the U.S. Department of Energy's Aquatic Species Program: Biodiesel From Algae; Close-Out Report, 1998. Golden, CO.
[17] K.R. Sawant, et al., One cell-two wells bio-refinery: demonstrating cyanobacterial chassis for co-production of heterologous and natural hydrocarbons, Bioresour. Technol. 363 (2022) 127921.
[18] S. Pacala, et al., Negative Emissions Technologies and Reliable Sequestration: A Research Agenda, The National Academies Press, Washington, DC, 2018.
[19] N. Hajinajaf, A. Mehrabadi, O. Tavakoli, Practical strategies to improve harvestable biomass energy yield in microalgal culture: a review, Biomass Bioenergy 145 (2021) 105941.
[20] Fallahi, A., et al., Effects of simultaneous CO2 addition and biomass recycling on growth characteristics of microalgal mixed culture. J. Chem. Technol. Biotechnol.
[21] S.A. Razzak, et al., Integrated CO2 capture, wastewater treatment and biofuel production by microalgae culturing—a review, Renew. Sust. Energ. Rev. 27 (2013) 622–653.
[22] Asgharnejad, H., et al., Comprehensive review of water management and wastewater treatment in food processing industries in the framework of water-food-environment nexus. Compr. Rev. Food Sci. Food Saf.
[23] A. Malek, L.C. Zullo, P. Daoutidis, Modeling and dynamic optimization of microalgae cultivation in outdoor open ponds, Ind. Eng. Chem. Res. 55 (12) (2016) 3327–3337.
[24] R.J. Wicker, et al., The potential of mixed-species biofilms to address remaining challenges for economically-feasible microalgal biorefineries: a review, Chem. Eng. J. 451 (2023) 138481.
[25] M.R. Tredici, Mass production of microalgae: photobioreactors, in: Handbook of Microalgal Culture: Biotechnology and Applied Phycology 1, 2004, pp. 178–214.
[26] L. Novoveská, et al., Overview and challenges of large-scale cultivation of photosynthetic microalgae and cyanobacteria, Mar. Drugs 21 (8) (2023) 445.
[27] A. Fallahi, et al., Cultivation of mixed microalgae using municipal wastewater: biomass productivity, nutrient removal, and biochemical content, Iran. J. Biotechnol. 18 (4) (2020) 88–97.
[28] F.G.A. Fernández, F.G. Camacho, Y. Chisti, Photobioreactors: light regime, mass transfer, and scaleup, in: Progress in Industrial Microbiology, Elsevier, 1999, pp. 231–247.
[29] E. Sierra, et al., Characterization of a flat plate photobioreactor for the production of microalgae, Chem. Eng. J. 138 (1–3) (2008) 136–147.
[30] J.S. Chang, et al., Photobioreactors, in: Current Developments in Biotechnology and Bioengineering, Elsevier, 2017, pp. 313–352.
[31] M. Talaei, A. Prieto, A review on performance of sustainable microalgae photobioreactor façades technology: exploring challenges and advantages, Archit. Sci. Rev. (2024) 1–28.
[32] E. Jacob-Lopes, et al., Development of operational strategies to remove carbon dioxide in photobioreactors, Chem. Eng. J. 153 (1–3) (2009) 120–126.
[33] L.G. Ramírez-Méridaet, et al., Why does the Photobioreactors Fail? J. Bioprocess. Biotech. (2015) 5–7, issue 7.
[34] H.-X. Chang, et al., Kinetic characteristics and modeling of microalgae Chlorella vulgaris growth and CO2 biofixation considering the coupled effects of light intensity and dissolved inorganic carbon, Bioresour. Technol. 206 (2016) 231–238.
[35] M.J. Barbosa, et al., Hypes, hopes, and the way forward for microalgal biotechnology, Trends Biotechnol. 41 (3) (2023) 452–471.
[36] L. Brennan, P. Owende, Biofuels from microalgae—a review of technologies for production, processing, and extractions of biofuels and co-products, Renew. Sust. Energ. Rev. 14 (2) (2010) 557–577.
[37] R. Craggs, D. Sutherland, H. Campbell, Hectare-scale demonstration of high rate algal ponds for enhanced wastewater treatment and biofuel production, J. Appl. Phycol. 24 (3) (2012) 329–337.
[38] D.L. Sutherland, et al., Seasonal variation in light utilisation, biomass production and nutrient removal by wastewater microalgae in a full-scale high-rate algal pond, J. Appl. Phycol. 26 (3) (2014) 1317–1329.
[39] K. Livansky, Losses of CO2 in outdoor mass algal cultures: determination of the mass transfer coefficient KL by means of measured pH course in NaHCO3 solution, Arch. Hydrobiol. Suppl. Unters. Elbe-Aestuars 85 (1990) 87–97.
[40] D.T. Van Arragon, Development of an Effective Process Model for Algae Growth in Photobioreactors, 2014.

[41] J. Villadsen, J. Nielsen, G. Lidén, Gas–liquid mass transfer, in: Bioreaction Engineering Principles, Springer, 2011, pp. 459–496.
[42] B.T. Nguyen, B.E. Rittmann, Effects of inorganic carbon and pH on growth kinetics of Synechocystis sp. PCC 6803, Algal Res. 19 (2016) 363–369.
[43] B. Wang, C.Q. Lan, M. Horsman, Closed photobioreactors for production of microalgal biomasses, Biotechnol. Adv. 30 (4) (2012) 904–912.
[44] Z. Chi, et al., Bicarbonate-based integrated carbon capture and algae production system with alkalihalophilic cyanobacterium, Bioresour. Technol. 133 (2013) 513–521.
[45] A.M. Santos, et al., Biomass and lipid productivity of Neochloris oleoabundans under alkaline–saline conditions, Algal Res. 2 (3) (2013) 204–211.
[46] A. Vadlamani, et al., High productivity cultivation of microalgae without concentrated CO2 input, ACS Sustain. Chem. Eng. 7 (2) (2018) 1933–1943.
[47] Y. Chen, et al., Integration of waste valorization for sustainable production of chemicals and materials via algal cultivation, in: Chemistry and Chemical Technologies in Waste Valorization, 2018, pp. 151–188.
[48] B.M. Hopkinson, C. Meile, C. Shen, Quantification of extracellular carbonic anhydrase activity in two marine diatoms and investigation of its role, Plant Physiol. 162 (2) (2013) 1142–1152.
[49] R. Prasad, et al., Role of microalgae in global CO2 sequestration: physiological mechanism, recent development, challenges, and future prospective, Sustainability 13 (23) (2021) 13061.
[50] D. Li, et al., Enhancing photosynthetic CO2 fixation by assembling metal-organic frameworks on Chlorella pyrenoidosa, Nat. Commun. 14 (1) (2023) 5337.
[51] E.V. Kupriyanova, N.A. Pronina, D.A. Los, Adapting from low to high: an update to CO2-concentrating mechanisms of cyanobacteria and microalgae, Plants 12 (7) (2023) 1569.
[52] S. Fal, A. Smouni, H. El Arroussi, Integrated microalgae-based biorefinery for wastewater treatment, industrial CO2 sequestration and microalgal biomass valorization: a circular bioeconomy approach, Environ. Adv. 12 (2023) 100365.
[53] Y.-D. Ding, et al., Dynamic behaviour of the CO2 bubble in a bubble column bioreactor for microalgal cultivation, Clean Techn. Environ. Policy 18 (7) (2016) 2039–2047.
[54] Y. Huang, et al., Optimizing the gas distributor based on CO2 bubble dynamic behaviors to improve microalgal biomass production in an air-lift photo-bioreactor, Bioresour. Technol. 233 (2017) 84–91.
[55] N. Azhand, A. Sadeghizadeh, R. Rahimi, Effect of superficial gas velocity on CO2 capture from air by Chlorella vulgaris microalgae in an airlift photobioreactor with external sparger, J. Environ. Chem. Eng. 8 (4) (2020) 104022.
[56] Y.-D. Ding, et al., Dynamic behaviour of the CO2 bubble in a bubble column bioreactor for microalgal cultivation, Clean Techn. Environ. Policy 18 (7) (2016) 2039–2047.
[57] L. Zhao, et al., Enhanced photo bio-reaction by multiscale bubbles, Chem. Eng. J. 354 (2018) 304–313.
[58] M. Barahoei, M.S. Hatamipour, S. Afsharzadeh, CO2 capturing by Chlorella vulgaris in a bubble column photo-bioreactor; effect of bubble size on CO2 removal and growth rate, J. CO2 Util. 37 (2020) 9–19.
[59] M. Anjos, et al., Optimization of CO2 bio-mitigation by Chlorella vulgaris, Bioresour. Technol. 139 (2013) 149–154.
[60] H.J. Ryu, K.K. Oh, Y.S. Kim, Optimization of the influential factors for the improvement of CO2 utilization efficiency and CO2 mass transfer rate, J. Ind. Eng. Chem. 15 (4) (2009) 471–475.
[61] D. Tang, et al., CO2 biofixation and fatty acid composition of Scenedesmus obliquus and Chlorella pyrenoidosa in response to different CO2 levels, Bioresour. Technol. 102 (3) (2011) 3071–3076.
[62] H.B. Hariz, et al., CO 2 fixation capability of Chlorella sp. and its use in treating agricultural wastewater, J. Appl. Phycol. 30 (6) (2018) 3017–3027.
[63] Y.-D. Ding, et al., Effect of CO2 bubbles behaviors on microalgal cells distribution and growth in bubble column photobioreactor, Int. J. Hydrog. Energy 41 (8) (2016) 4879–4887.
[64] Y.S. Lai, et al., Achieving superior carbon transfer efficiency and pH control using membrane carbonation with a wide range of CO2 contents for the coccolithophore Emiliania huxleyi, Sci. Total Environ. 822 (2022) 153592.
[65] S. Zhao, et al., Experimental and theoretical study on dissolution of a single mixed gas bubble in a microalgae suspension, RSC Adv. 5 (41) (2015) 32615–32625.
[66] J.L. Mendoza, et al., Oxygen transfer and evolution in microalgal culture in open raceways, Bioresour. Technol. 137 (2013) 188–195.
[67] E. Molina, et al., Tubular photobioreactor design for algal cultures, J. Biotechnol. 92 (2) (2001) 113–131.
[68] A. Kazbar, et al., Effect of dissolved oxygen concentration on microalgal culture in photobioreactors, Algal Res. 39 (2019) 101432.
[69] F.C. Rubio, et al., Prediction of dissolved oxygen and carbon dioxide concentration profiles in tubular photobioreactors for microalgal culture, Biotechnol. Bioeng. 62 (1) (1999) 71–86.
[70] S.-Y. Chiu, et al., Reduction of CO2 by a high-density culture of Chlorella sp. in a semicontinuous photobioreactor, Bioresour. Technol. 99 (9) (2008) 3389–3396.
[71] M.G. de Morais, J.A.V. Costa, Biofixation of carbon dioxide by Spirulina sp. and Scenedesmus obliquus cultivated in a three-stage serial tubular photobioreactor, J. Biotechnol. 129 (3) (2007) 439–445.
[72] C. Yoo, et al., Selection of microalgae for lipid production under high levels carbon dioxide, Bioresour. Technol. 101 (1) (2010) S71–S74.
[73] W. Tongprawhan, S. Srinuanpan, B. Cheirsilp, Biocapture of CO2 from biogas by oleaginous microalgae for improving methane content and simultaneously producing lipid, Bioresour. Technol. 170 (2014) 90–99.
[74] E. Eustance, et al., Improved CO2 utilization efficiency using membrane carbonation in outdoor raceways, Algal Res. 51 (2020) 102070.
[75] H.-W. Kim, J. Cheng, B.E. Rittmann, Direct membrane-carbonation photobioreactor producing photoautotrophic biomass via carbon dioxide transfer and nutrient removal, Bioresour. Technol. 204 (2016) 32–37.
[76] G.D. Okcu, et al., Evaluation of co-culturing a diatom and a coccolithophore using different silicate concentrations, Sci. Total Environ. 769 (2021) 145217.
[77] J.P. Bitog, et al., Application of computational fluid dynamics for modeling and designing photobioreactors for microalgae production: a review, Comput. Electron. Agric. 76 (2) (2011) 131–147.
[78] C.U. Ugwu, H. Aoyagi, H. Uchiyama, Photobioreactors for mass cultivation of algae, Bioresour. Technol. 99 (10) (2008) 4021–4028.
[79] P. Wongsuchoto, T. Charinpanitkul, P. Pavasant, Bubble size distribution and gas–liquid mass transfer in airlift contactors, Chem. Eng. J. 92 (1–3) (2003) 81–90.
[80] L.C. Mutharasu, et al., Experimental study and CFD simulation of the multiphase flow conditions encountered in a Novel Down-flow bubble column, Chem. Eng. J. 350 (2018) 507–522.
[81] G. Besagni, L. Gallazzini, F. Inzoli, On the scale-up criteria for bubble columns, Petroleum 5 (2) (2019) 114–122.
[82] J.C.M. Pires, M.C.M. Alvim-Ferraz, F.G. Martins, Photobioreactor design for microalgae production through computational fluid dynamics: a review, Renew. Sust. Energ. Rev. 79 (2017) 248–254.
[83] R. Bronnenmeier, H. Märkl, Hydrodynamic stress capacity of microorganisms, Biotechnol. Bioeng. 24 (3) (1982) 553–578.
[84] H.J. Silva, T. Cortifas, R.J. Ertola, Effect of hydrodynamic stress on Dunaliella growth, J. Chem. Technol. Biotechnol. 40 (1) (1987) 41–49.
[85] P. Jaouen, L. Vandanjon, F. Quéméneur, The shear stress of microalgal cell suspensions (Tetraselmis suecica) in tangential flow filtration systems: the role of pumps, Bioresour. Technol. 68 (2) (1999) 149–154.
[86] W.H. Thomas, C.H. Gibson, Effects of small-scale turbulence on microalgae, J. Appl. Phycol. 2 (1) (1990) 71–77.
[87] D. Rosso, M.K. Stenstrom, M. Garrido-Baserba, Aeration and Mixing, 2020.
[88] ISO. 2017. p. 20480-1:2017(en).
[89] Q. Wang, et al., Generation and stability of size-adjustable bulk nanobubbles based on periodic pressure change, Sci. Rep. 9 (1) (2019) 1–9.
[90] J.J. Baker, Minimizing Optimal CO2 Feed to Algal Cultures Utilizing Microfluidic Devices Generating Micon-sized Bubbles, Johns Hopkins University, 2015.
[91] W.B. Zimmerman, V. Tesař, H.C.H. Bandulasena, Towards energy efficient nanobubble generation with fluidic oscillation, Curr. Opin. Colloid Interface Sci. 16 (4) (2011) 350–356.
[92] A.K. Patel, et al., Advances in micro-and nano bubbles technology for application in biochemical processes, Environ. Technol. Innov. 23 (2021) 101729.
[93] N.T. Eriksen, B.R. Poulsen, J.J. Lønsmann Iversen, Dual sparging laboratory-scale photobioreactor for continuous production of microalgae, J. Appl. Phycol. 10 (4) (1998) 377–382.
[94] C.R. Branan, Rules of Thumb for Chemical Engineers: Manual of Quick, Accurate Solutions to Everyday Process Engineering Problems, Gulf Professional Pub, 2002.
[95] K. Wongwailikhit, et al., Gas Sparger orifice sizes and solid particle characteristics in a bubble column–relative effect on hydrodynamics and mass transfer, Chem. Eng. Technol. 41 (3) (2018) 461–468.
[96] N. De Nevers, G.D. Silcox, Fluid Mechanics for Chemical Engineers, McGraw-Hill New York, 1991.
[97] G. Li, et al., Hydrodynamics, mass transfer and cell growth characteristics in a novel microbubble stirred bioreactor employing sintered porous metal plate impeller as gas sparger, Chem. Eng. Sci. 192 (2018) 665–677.
[98] V.V. Buwa, V.V. Ranade, Dynamics of gas–liquid flow in a rectangular bubble column: experiments and single/multi-group CFD simulations, Chem. Eng. Sci. 57 (22–23) (2002) 4715–4736.
[99] M. Polli, et al., Bubble size distribution in the sparger region of bubble columns, Chem. Eng. Sci. 57 (1) (2002) 197–205.
[100] J.O. Hanotu, H. Bandulasena, W.B. Zimmerman, Aerator design for microbubble generation, Chem. Eng. Res. Des. 123 (2017) 367–376.
[101] S. Katuwal, Designing and Development of a Photobioreactor for Optimizing the Growth of Micro Algae and Studying Its Growth Parameters, 2017.
[102] R. Putt, et al., An efficient system for carbonation of high-rate algae pond water to enhance CO2 mass transfer, Bioresour. Technol. 102 (3) (2011) 3240–3245.
[103] C. Molina-Fernández, P. Luis, Immobilization of carbonic anhydrase for CO2 capture and its industrial implementation: a review, J. CO2 Util. 47 (2021) 101475.
[104] J. Shen, Y. Yuan, S. Salmon, Carbonic anhydrase immobilized on textile structured packing using chitosan entrapment for CO2 capture, ACS Sustain. Chem. Eng. 10 (23) (2022) 7772–7785.
[105] D.T. Arazawa, et al., Immobilized carbonic anhydrase on hollow fiber membranes accelerates CO2 removal from blood, J. Membr. Sci. 403 (2012) 25–31.
[106] X. Xu, S.E. Kentish, G.J.O. Martin, Direct air capture of CO2 by microalgae with buoyant beads encapsulating carbonic anhydrase, ACS Sustain. Chem. Eng. 9 (29) (2021) 9698–9706.
[107] H. Bose, T. Satyanarayana, Microbial carbonic anhydrases in biomimetic carbon sequestration for mitigating global warming: prospects and perspectives, Front. Microbiol. 8 (2017) 1615.
[108] J. Cheng, et al., A novel jet-aerated tangential swirling-flow plate photobioreactor generates microbubbles that enhance mass transfer and improve microalgal growth, Bioresour. Technol. 288 (2019) 121531.
[109] V. Mortezaeikia, R. Yegani, O. Tavakoli, Membrane-sparger vs. membrane contactor as a photobioreactors for carbon dioxide biofixation of Synechococcus elongatus in batch and semi-continuous mode, J. CO2 Util. 16 (2016) 23–31.

[110] H. Zheng, et al., Effect of CO2 supply conditions on lipid production of Chlorella vulgaris from enzymatic hydrolysates of lipid-extracted microalgal biomass residues, Bioresour. Technol. 126 (2012) 24–30.
[111] J.-M. Lv, et al., Enhanced lipid production of Chlorella vulgaris by adjustment of cultivation conditions, Bioresour. Technol. 101 (17) (2010) 6797–6804.
[112] A.L. Gonçalves, et al., The effect of increasing CO2 concentrations on its capture, biomass production and wastewater bioremediation by microalgae and cyanobacteria, Algal Res. 14 (2016) 127–136.
[113] M.K. Lam, K.T. Lee, Effect of carbon source towards the growth of Chlorella vulgaris for CO2 bio-mitigation and biodiesel production, Int. J. Greenh. Gas Control 14 (2013) 169–176.
[114] M. Shabani, CO2 bio-sequestration by Chlorella vulgaris and Spirulina platensis in response to different levels of salinity and CO2, Proc. Int. Acad. Ecol. Environ. Sci. 6 (2) (2016) 53.
[115] V.R. Naira, D. Das, S.K. Maiti, Real time light intensity based carbon dioxide feeding for high cell-density microalgae cultivation and biodiesel production in a bubble column photobioreactor under outdoor natural sunlight, Bioresour. Technol. 284 (2019) 43–55.
[116] J. Cheng, et al., Strengthening mass transfer of carbon dioxide microbubbles dissolver in a horizontal tubular photo-bioreactor for improving microalgae growth, Bioresour. Technol. 277 (2019) 11–17.
[117] M. Derakhshandeh, U.T. Un, Optimization of microalgae Scenedesmus SP. growth rate using a central composite design statistical approach, Biomass Bioenergy 122 (2019) 211–220.
[118] C.A. Arroyo, et al., CO2 capture of the gas emission, using a catalytic converter and airlift bioreactors with the microalga Scenedesmus dimorphus, Appl. Sci. 9 (16) (2019) 3212.
[119] J. Piiparinen, et al., Microalgal CO2 capture at extreme pH values, Algal Res. 32 (2018) 321–328.
[120] B.N. Thorat, A.V. Kulkarni, J.B. Joshi, Design of sieve plate spargers for bubble columns: role of weeping, Chem. Eng. Technol. 24 (8) (2001) 815–828.
[121] A.V. Kulkarni, S.S. Roy, J.B. Joshi, Pressure and flow distribution in pipe and ring spargers: experimental measurements and CFD simulation, Chem. Eng. J. 133 (1–3) (2007) 173–186.
[122] A.V. Kulkarni, S.V. Badgandi, J.B. Joshi, Design of ring and spider type spargers for bubble column reactor: experimental measurements and CFD simulation of flow and weeping, Chem. Eng. Res. Des. 87 (12) (2009) 1612–1630.
[123] A.V. Kulkarni, J.B. Joshi, Design and selection of sparger for bubble column reactor. Part I: performance of different spargers, Chem. Eng. Res. Des. 89 (10) (2011) 1972–1985.
[124] K.A. Falinski, et al., Response of Tisochrysis lutea [Prymnesiophycidae] to aeration conditions in a bench-scale photobioreactor, J. Appl. Phycol. 30 (4) (2018) 2203–2214.
[125] Q. Zheng, G.J.O. Martin, S.E. Kentish, Energy efficient transfer of carbon dioxide from flue gases to microalgal systems, Energy Environ. Sci. 9 (3) (2016) 1074–1082.
[126] E. Eustance, et al., Volatile nutrients-improving utilization of ammonia and carbon dioxide in microalgal cultivation: a review, Curr. Biotechnol. 5 (2) (2016) 130–141.